Published by Institute of Physics Publishing for SISSA
Received: *September 22, 2005*
Accepted: *October 15, 2005*
Published: *October 24, 2005*

Study of perturbative QCD predictions at next-to-leading order and beyond for $\mathrm{pp} \to \mathrm{H} \to \gamma\gamma + X$

Fabian Stöckli, André G. Holzner and Günther Dissertori

Institute for Particle Physics
ETH Zurich, CH-8093 Zurich, Switzerland
E-mail: Fabian.Stoeckli@cern.ch, Andre.Georg.Holzner@cern.ch, Guenther.Dissertori@cern.ch

Abstract: We study predictions from perturbative Quantum Chromodynamics (QCD) for the process $\mathrm{pp} \to \mathrm{H} \to \gamma\gamma+X$. In particular, we compare fully differential calculations at next-to-leading (NLO) and next-to-next-to-leading order (NNLO) in the strong coupling constant to the results obtained with the MC@NLO Monte Carlo (MC) generator, which combines QCD matrix elements at NLO with a parton shower algorithm. Estimates for the systematic uncertainties in the various predictions due to the choice of the renormalization scale and the parton distribution functions are given for the inclusive and accepted cross sections and for the corresponding acceptance corrections, obtained after applying standard selection and acceptance cuts. Furthermore, we compare the distributions for the Higgs signal to those for the irreducible two-photon background, obtained with a NLO MC simulation.

Keywords: Hadron-Hadron Scattering, QCD, NLO Computations, Higgs Physics.

Contents

1. Introduction

One of the main goals of the future Large Hadron Collider (LHC) at CERN is the search for the Higgs boson. From theoretical considerations [1] it is concluded that the Higgs mass should be below about one TeV/c^2. In addition, precision measurements of electroweak observables [2] indicate that the low-mass region (approximately below 200 GeV/c^2) is preferred. If the Higgs boson mass is smaller than twice the W mass, its decay mode into a pair of photons will be among the most important and distinct channels for the Higgs search. Since this decay can only proceed via loop corrections, the corresponding branching ratio is less than one percent. However, it provides the experimentally cleanest signature [3 – 5].

Obviously, one important aspect of the preparations for the upcoming LHC Higgs searches is to study the predictions for the distributions of kinematic variables for the signal, pp $\rightarrow$ H $\rightarrow \gamma\gamma + X$, and the background processes (eg. pp $\rightarrow \gamma\gamma + X$), obtained from perturbative Quantum Chromodynamics (QCD). It is known that the inclusive Higgs cross section gets large perturbative corrections at next-to-leading order (NLO) [6 – 9] and next-to-next-to-leading order (NNLO) [10 – 14], so it is likely that the dynamics of the process is different at various orders in perturbation theory. That is, the QCD corrections to the production process change the kinematics of the Higgs boson and lead to modifications in the kinematics of the final-state photons. It is worth noting here that very recently the leading threshold-enhanced third-order (N^3LO) corrections to the total Higgs cross section have been derived [15], showing that the perturbative expansion stabilizes. Furthermore, at the level of precision reached by the NNLO calculations, it might become relevant to consider also electro-weak corrections, which have been computed at two-loop approximation for the Higgs production [16] and decay [17].

The detailed knowledge of differential cross sections will help to optimize the search strategy and thus improve the signal over background ratio. In the past, such studies have been performed using leading order (LO) Monte Carlo generators, which usually include a parton shower and a hadronization model and are finally combined with a full detector simulation. Higher order QCD predictions in general were only available for the inclusive cross sections or for distributions of some kinematic variable of the Higgs boson, for example its transverse momentum, $p_{\rm T}$ [18, 19]. Therefore, the K-factors applied to the LO predictions to correct for the missing higher order terms would not take account of the analysis selection and acceptance cuts, which might reduce the allowed phase space in a non-trivial way. An attempt to improve on this consists in a re-weighting procedure where the LO plus parton shower results are re-scaled in order to reproduce the higher order prediction for a particular kinematic variable, such as the Higgs $p_{\rm T}$. Taking account of these weights and of the efficiencies obtained from the MC simulation, an effective K-factor can be computed which incorporates the selection and acceptance factors [20].

Recently, new calculations for the process pp $\rightarrow$H $\rightarrow\gamma\gamma + X$ beyond NLO have become available, which now allow for an analysis of acceptance corrections and the related systematic uncertainties at higher order in perturbative QCD. In particular, the fully differential cross section at NNLO has been computed for the first time [21, 22], giving the exact expressions (up to this order of perturbative QCD) for Higgs production and its two-photon decay with up to two additional massless partons (quarks or gluons). Therefore this new semi-analytical calculation allows to apply realistic selection and isolation cuts to the Higgs decay products and the additional partons in the final state, as well as to study the distributions of relevant kinematic variables, such as the rapidity and $p_{\rm T}$ of the Higgs and the photons, at NNLO accuracy.

An alternative approach consists in the combination of QCD matrix elements at NLO and a parton shower algorithm, therefore taking into account also large logarithms due to soft and collinear radiation at all orders in the strong coupling constant. This is implemented in the Monte Carlo (MC) generator MC@NLO [23, 24], combined with the HERWIG MC program [25, 26], which in addition handles the hadronization process and particle decays. Several aspects render such an approach interesting for phenomenological studies and experimental analyses. In contrast to a pure parton level calculation, such a MC generator allows to investigate distributions at the particle (hadrons and leptons) level, which is closer to the actually measured final state than partons. For example, the detailed internal structure of jets is modeled rather well, studies of lepton isolation from jets are expected to be more realistic and it is possible to simulate also the effects of the underlying event and multiple interactions. Finally, it is rather straightforward to feed the output of this generator into a full detector simulation, which is necessary for the experimenter in order to develop optimised data analyses which rely on a good approximation of the

JHEP10(2005)079

underlying QCD dynamics. There is already a considerable list of processes available in MC@NLO, among these pp $\rightarrow$H $\rightarrow\gamma\gamma + X$, and further additions can be expected in the future.

This paper provides a first detailed comparison of these newly available predictions. Taking the various calculations, we apply standard cuts to relevant kinematic observables in order to reproduce in a realistic manner the basic aspects of the Higgs search in the two-photon channel at LHC. As a result, we are able to compare the predictions for the inclusive and accepted cross sections, as well as for the corresponding acceptance corrections. These comparisons are done as a function of the Higgs mass and the renormalization/factorization scales. In addition, we study the dependence of the MC@NLO predictions on the choice of the parton distribution functions (pdf). Regarding the latter, it can be interesting to compare the predictions when combining MC@NLO with pdfs extracted at NLO as well as at NNLO accuracy. Although via the combination of NLO matrix elements with the initial state parton shower effectively also terms beyond NLO are generated for the perturbative part of the scattering process, the use of NNLO pdfs in MC@NLO should be regarded as equivalent to that of NLO pdfs, since, formally, the accuracy of the results is NLO in both cases.

Interesting kinematic observables of the two-photon final state, as proposed in [27] and [22], are computed for the signal as well as for the irreducible two-photon background, pp $\rightarrow\gamma\gamma+X$. The latter is known at NLO accuracy [27, 28]. It is shown that variables such as the average photon transverse momentum or the rapidity difference of the two photons could contribute to the discrimination of the signal from the background.

It is worth noting that the entire study is done at the phenomenological level, i.e. no attempt is made here to simulate any detector effects beyond the basic selection criteria, such as acceptance cuts in photon rapidity and transverse momentum, as well as isolation requirements. We thus emphasize that this paper does not provide a re-evaluation of the Higgs discovery potential at LHC, but rather intends to show the level of theoretical accuracy, which is achievable with the tools that have become available recently, as well as to indicate where more detailed studies, including full detector simulation and the most up-to-date perturbative QCD predictions, might be worthwhile pursuing.

The paper is organized as follows: In section 2 we list the details on the computer programs and the relevant parameter settings which were used to perform this study. In section 3 the basic event selection cuts are described. The resulting cross sections before and after this selection are discussed in section 4 and the distributions of some kinematic variables are presented in section 5. The comparison to the main background is given in section 6. Finally, section 7 contains a summary of the results.

2. Computer programs and parameter settings

In order to carry out this study we have used several different software packages, which implement the various signal and background predictions up to a certain level of approximation in perturbation theory. The employed programs are :

- FEHIP [22] (Version 1.0)
  This code is used to calculate the fully differential cross section for Higgs boson production through gluon fusion at NLO and NNLO QCD, in the narrow-width approximation. The gluon fusion channel via a top quark loop contributes a fraction of about 80% to the total Higgs production cross section in the relevant low-mass region. The calculation has been carried out in the limit of an infinitely heavy top quark, in which the Higgs boson coupling to gluons is point-like. However, the results are re-scaled using the ratio of the LO cross section predictions, obtained with the exact top mass dependence and in the heavy top mass limit. As discussed in [22], this gives an excellent approximation.

  For the consistent convolution of the partonic cross sections at NLO (NNLO) with parton distribution functions, the MRST01 NLO (NNLO) [29] pdf sets are used. The so-called MODE 1 is employed as the default mode for pdf evolution. For the moment being, no other pdf set is available with this program and we have made no attempt to include further sets.

  The code returns the four-momenta of the Higgs boson and the final state particles, namely two photons and up to two additional massless partons, which can be used to evaluate an analysis function for every event. This analysis function is then convoluted with the squared matrix elements of the corresponding final state in order to finally obtain a cross section. Many of the numerical results, in particular at NNLO, were obtained from [30, 22]. Concerning statistical uncertainties, the NNLO results for the cross sections (acceptance corrections) are accurate to 1% (2%), while the NLO numbers have been computed up to an accuracy of 0.1%.

  In order to speed up the computation, for the Monte Carlo integration step a parallel VEGAS algorithm has been used [31, 32]. The available C++ code has been slightly modified in order to meet the specific needs of FEHIP. The code has been parallelized using the Standard Message Passing Interface MPI [33].

- MC@NLO [23, 24] (Version 2.31)
  As described in the introduction, this MC generator consistently incorporates NLO QCD matrix elements into a parton shower framework. In the purely inclusive case the code returns the NLO cross section, whereas the effects of the parton shower become only apparent when cuts are applied to the final state. In order to eliminate a problem with this version of the code when using renormalization and factorization scales that differ from the default choice ($\mu = m_{\rm H}$), a correction has been applied [34].

  MC@NLO is used together with the HERWIG event generator [25, 26], which handles the simulation of the parton shower, the hadronization process and possible particle decays. The exact top mass dependence is retained at the Born level. We have generated events using three different pdf sets. In addition to the two MRST01 sets mentioned above, we have also used the CTEQ6M [35] set, which has been extracted at NLO accuracy.

- DIPHOX [28] (Version 1.2)
  The background process pp $\rightarrow\gamma\gamma + X$ is computed with this program, which provides a NLO QCD prediction at parton level only. The (unphysical) phase-space slicing parameter $p_{\mathrm{T_m}}$ [28] was set to 0.05 GeV/c. An additional contribution to this process, which is not included in DIPHOX, namely the two-loop correction to the gluon fusion subprocess, has been calculated in [27]. There it is shown that this contribution is modest, around 10% or smaller for the mass range of interest in the low-mass Higgs search.

- HDECAY [36] (Version 3.101)
  This is used to calculate the branching ratio of the Higgs decay to two photons, resulting in BR(H $\rightarrow\gamma\gamma$) = 0.22 %.

- HIGLU [37] (Version 2.102)
  The program HIGLU allows to calculate the inclusive cross section for Higgs boson production through gluon fusion at NLO, with the exact top mass dependence at both LO and NLO.

Throughout this analysis a top mass of $m_{\mathrm{top}} = 175$ GeV/c^2 has been assumed. Whenever we refer to 'the scale' μ, it means $\mu = \mu_{\mathrm{R}} = \mu_{\mathrm{F}}$, i.e. the factorization and renormalization scales are set to the same value.

3. Event selection

In this study we attempt to simulate in an appropriate manner the planned Higgs searches at LHC in the two-photon channel, using only phenomenological, i.e. parton and/or particle level, predictions without any detailed detector simulation. This is achieved by taking into account the geometrical limitations of a typical LHC detector and the foreseen trigger requirements. Furthermore, in order to reduce the large irreducible background the following cuts are applied to the final state photons :

- The absolute value of the pseudorapidity $|\eta_{\gamma_{1,2}}|$ of each of the two photons must be smaller than 2.5. This corresponds to the coverage in polar angle of a detector such as ATLAS [38] or CMS [39].

- One of the two photons must have a transverse energy above 40 GeV, while the other photon is required to have a transverse energy above 25 GeV.

- In order to exclude events with considerable hadronic activity around the final state photons, as for example can be expected in background events with quark-photon fragmentation, the photons must be isolated, i.e. the additional energy in a cone $\Delta R = \sqrt{\Delta\eta^2 + \Delta\varphi^2} < 0.4$ around each photon must not exceed 15 GeV.

This selection is basically the same as the 'standard cone criterion' used in [27]. For reasons given in that reference (e.g. calorimeter granularity and finite photon shower size),

JHEP10(2005)079

we did not investigate the smooth cone isolation criterion [40]. In the following, we will refer to these selection cuts as the 'standard cuts' and call the accepted photon with the highest (second highest) transverse energy photon 1 (photon 2).

4. Inclusive and accepted cross sections

In the following section we study the predictions at various orders in perturbative QCD for the inclusive pp $\to$H $\to\gamma\gamma + X$ cross section $\sigma_{\rm inc}$, as well as for the accepted cross section $\sigma_{\rm acc}$ found after the standard cuts on the final state photons have been applied. The comparison is made for several different choices of parameters, such as the Higgs mass, the scale or the pdf set. For the moment we simply assume that the branching ratio of the Higgs decay into two photons is one.

In a first step, we fix the Higgs mass to $m_{\rm H} = 120$ GeV/c^2, the factorization scale $\mu_{\rm F}$ and renormalization scale $\mu_{\rm R}$ are set to $m_{\rm H}/2$ and the pdfs are taken from the MRST01 set, using the NLO (NNLO) pdfs in combination with MC@NLO and FEHIP at NLO (NNLO). As discussed in detail in ref. [22], the choice $\mu_{\rm F} = \mu_{\rm R} = m_{\rm H}/2$ is motivated by the observation of an improved convergence of the perturbation series and the very good agreement with the threshold-resummed results for the Higgs hadroproduction cross section [41]. This is further confirmed by the recent calculation of the threshold-enhanced third-order corrections [15].

The results can be found in table 1. Whereas with MC@NLO we give the acceptances for each single cut as well as for groups of cuts, in the case of FEHIP we had to restrict ourselves to the acceptance after all cuts, since this NNLO code is very cpu-intensive. Regarding the inclusive cross section, $\sigma_{\rm inc}$, we observe that the MC@NLO prediction falls short of the NLO prediction of FEHIP by about 3.3%. By construction MC@NLO should return the exact NLO cross section if no cuts are applied. Thus the observed difference has to be explained by the different treatment of the top mass dependence. FEHIP uses the infinite top mass limit in all orders of the calculation and then re-scales the result using the ratio of the exact and approximated ($m_{\rm top} \to \infty$) LO cross sections, while MC@NLO keeps the exact top mass dependence at LO, but uses the $m_{\rm top} \to \infty$ approximation at NLO. For comparison, the result obtained with HIGLU which retains the exact top mass dependence at LO and NLO is $\sigma_{\rm inc} = 44.39 \pm 0.01$ pb. Thus FEHIP returns a 0.9% higher and MC@NLO a 2.5% lower NLO cross section with respect to HIGLU.

The differences of the NLO results with respect to the NNLO result amount to 13% (MC@NLO) and 9% (FEHIP, NLO). After the standard selection, these differences are reduced to about 10% and 6%, respectively. The acceptance corrections for $m_{\rm H} = 120$ GeV/c^2, defined as the ratio between the accepted and the inclusive cross sections, $\sigma_{\rm acc}/\sigma_{\rm inc}$, agree to within 2% (absolute).

It turns out that the NNLO calculation predicts a slightly stronger reduction in the accepted cross section than the other two approaches. With the MC@NLO generator we have also studied the effect of the individual cuts. We find that the reduction in cross section is mainly due to the angular and momentum cuts, whereas the isolation requirement has only a very minor impact.

JHEP10(2005)079

4.1 Choice of pdfs in MC@NLO

As a first variation with respect to the parameter choices given above, we investigate the dependence on the pdfs used together with MC@NLO. Since MC@NLO includes the leading effects of soft and collinear radiation to all orders, thus beyond NLO, it is interesting to combine it with the NNLO pdf set of the MRST01 fits, which has been extracted using a combination of NLO and NNLO cross sections. Finally, we also take CTEQ6M (NLO) as input, in order to study an alternative set of pdfs, obtained under different assumptions, from a somewhat different data set and thus with different theoretical and experimental systematic uncertainties.

The results are listed in table 1. Compared to MRST01 NLO, the results found with the MRST01 NNLO set, for both $\sigma_{\rm inc}$ and $\sigma_{\rm acc}$, differ quite considerably, up to 16%, whereas the cross sections obtained with the NLO sets from the MRST01 and CTEQ6M fits agree to better than 4%. The considerably lower cross sections obtained with the NNLO set are interpreted as arising from the smaller gluon density and strong coupling used in this set. It is worth noting that in the NNLO calculation, as implemented in FEHIP, the NNLO corrections in the matrix elements, which also include additional scale dependent terms, counter the effect of the NNLO evolution of the pdfs.

Interestingly, when looking at the acceptance, we find agreement for all three choices within 1.1%, absolute; when also considering the FEHIP results the span between the largest and smallest acceptance increases to 2.3%. Half of this span could be defined as a 1.8% 'uncertainty' relative to the average of the largest and smallest values. Calculating the same relative uncertainty for the accepted cross section, we find 4.7%. Thus the acceptance correction is less sensitive with respect to the choice of pdfs and the approximations made by the perturbative calculation than the absolute cross section.

4.2 Variation of the Higgs mass

In table 2 the results are given for the inclusive and the accepted cross sections for different Higgs masses, obtained with MC@NLO and FEHIP (NNLO). The renormalization and factorization scales are chosen to be $\mu = m_{\rm H}/2$.

In the upper part of the table the inclusive cross sections $\sigma_{\rm inc}$ for MC@NLO (MRST01 NLO) and the NNLO results obtained with FEHIP (MRST01 NNLO) are compared. It can be observed that the inclusive cross sections obtained with MC@NLO are 16% smaller than the NNLO results for the full Higgs mass range investigated here. In the second part of table 2 the MC@NLO predictions for the acceptance corrections, after the various cuts, are given. As stated above, the isolation cut has the smallest effect on the acceptance corrections. The increased acceptance of the cuts on $p_{\rm T}$ and η when increasing the Higgs mass arises from the higher transverse momenta expected in this region. Therefore also the total acceptance increases with larger $m_{\rm H}$. The results after cuts, obtained with MC@NLO and FEHIP, agree to within 11%. This reduced difference compared to the inclusive case is due to the slightly larger acceptance correction found with MC@NLO. Remarkably, the acceptance corrections for MC@NLO and FEHIP (NNLO) agree within 3.2% (absolute) over the whole investigated mass range.

JHEP10(2005)079

Generator	MC@NLO			FEHIP NLO	FEHIP NNLO
PDF set	MRST NLO	MRST NNLO	CTEQ	MRST NLO	MRST NNLO
σ_{inc} [pb]	43.30	37.67	44.32	44.77	48.94
Acceptances ($\sigma_{\text{acc}}/\sigma_{\text{inc}}$) of single groups of cuts					
p_{T}-cuts	80.2 %	80.3 %	80.1 %		
η-cuts	83.2 %	83.0 %	83.8 %		
isolation	99.7 %	99.7 %	99.8 %		
Acceptances ($\sigma_{\text{acc}}/\sigma_{\text{inc}}$) of two groups of cuts					
p_{T}- and η-cuts	63.6 %	63.2 %	64.3 %		
p_{T}-cuts and isolation	79.6 %	79.7 %	79.6 %		
η-cuts and isolation	81.5 %	81.1 %	82.1 %		
All three groups of cuts					
Acceptance	63.0 %	62.6 %	63.7 %	63.4 %	61.4 %
σ_{acc} [pb]	27.30	23.60	28.25	28.35	30.07

Table 1: Cross sections and acceptance corrections for a Higgs mass of $m_{\text{H}} = 120$ GeV$/c^2$, obtained with MC@NLO and FEHIP (NLO and NNLO) for different cuts and pdf sets. The renormalization and factorization scale are set to $\mu = m_{\text{H}}/2$. The branching ratio H $\rightarrow\gamma\gamma$ is assumed to be one. The statistical uncertainties are at the one (two) per-cent level for the NNLO cross sections (acceptance) and negligible for the other cases.

Generator	MC@NLO	NNLO	MC@NLO	NNLO	MC@NLO	NNLO	MC@NLO	NNLO	MC@NLO	NNLO
m_{H} [GeV]	110		120		130		140		150	
σ_{inc}[pb]	50.65	56.82	43.30	48.94	37.45	42.54	32.66	37.37	28.70	33.10
Acceptances ($\sigma_{\text{acc}}/\sigma_{\text{inc}}$) of single groups of cuts										
p_{T}-cuts	75.9 %		80.2 %		83.3 %		85.9 %		87.8 %	
η-cuts	82.4 %		83.2 %		84.0 %		84.8 %		85.3 %	
isolation	99.7 %		99.7 %		99.7 %		99.7 %		99.7 %	
Acceptances ($\sigma_{\text{acc}}/\sigma_{\text{inc}}$) of two groups of cuts										
p_{T}- and η-cuts	59.9 %		63.6 %		66.3 %		68.6 %		70.5 %	
p_{T}-cuts and isolation	75.4 %		79.6 %		82.7 %		85.2 %		87.1 %	
η-cuts and isolation	80.7 %		81.5 %		82.1 %		82.8 %		83.3 %	
All three groups of cuts										
Acceptance	59.5 %	57.3 %	63.0 %	61.4 %	65.7 %	63.7 %	67.9 %	64.7 %	69.7 %	67.4 %
σ_{acc} [pb]	30.11	32.56	27.30	30.07	24.60	27.08	22.19	24.17	20.01	22.30

Table 2: Acceptance corrections for the different cuts and the different Higgs masses, as obtained with MC@NLO and FEHIP (NNLO). The used pdfs are MRST01 NLO for MC@NLO and MRST01 NNLO for FEHIP. The renormalization and factorization scales are set to $\mu = m_{\text{H}}/2$. The statistical uncertainties are at the one (two) per-cent level for the NNLO cross sections (acceptance) and negligible for the other cases.

The results are shown in figure 1, where the inclusive and accepted cross section, as well as the acceptance correction, are plotted as a function of m_{H}. It is worth noting that the statistical uncertainty of the NNLO results for the acceptance correction is at the 2% level.

4.3 Variation of the renormalization and factorization scale μ

Both the renormalization and factorization scales are un-physical variables which are introduced in the regularization step of the renormalization and/or factorization procedure,

JHEP10(2005)079

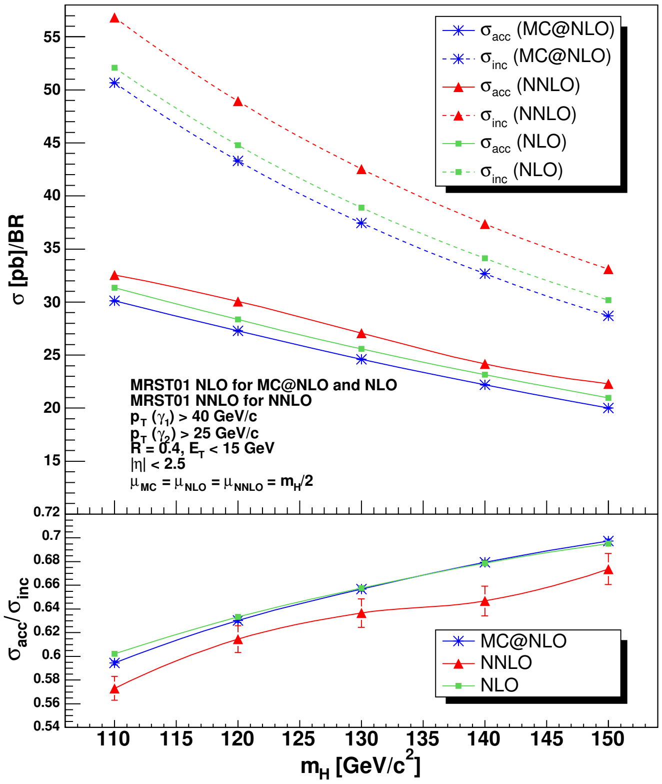

Figure 1: Inclusive and accepted cross sections as a function of the Higgs mass, m_{H}, obtained with MC@NLO and FEHIP (at NLO and NNLO).

which is needed to deal with the divergent integrals encountered in the perturbative calculations. An approximation for a perturbatively calculated observable, obtained to some order in the coupling constant, does not depend on these scales up to the calculated order, but a dependence appears at the next-higher order. It is thus interesting to investigate the remaining dependence of a given higher-order calculation. The range over which these scales are varied, and the usually quoted systematic uncertainties corresponding to the spread in the results when varying the scales, are somehow arbitrary and subject to controversy. For this analysis we have studied scale variations between $m_{\mathrm{H}}/4$ and $2\,m_{\mathrm{H}}$, in both MC@NLO and FEHIP. It is worth noting that other settings of the scales are possible in MC@NLO, for example, including some p_{T}-dependence. Our approach is convenient for a direct comparison of MC@NLO and FEHIP.

The NNLO results when choosing either $\mu = m_{\mathrm{H}}/2$ or $\mu = 2\,m_{\mathrm{H}}$ are shown in figure 2. As can be observed in figure 3, the NLO cross sections start to increase very rapidly when going to very small scales, whereas the scale dependence at NNLO is considerably flatter. The difference between the NLO predictions from FEHIP and MC@NLO can be explained by the different treatment of the top mass dependence.

For a Higgs mass of $m_{\mathrm{H}} = 120$ GeV$/c^2$, as used in figure 3, it appears that a range of scales between $m_{\mathrm{H}}/2$ and $2\,m_{\mathrm{H}}$ might be reasonable for evaluating a possible systematic uncertainty because of this effect. Table 3 summarizes the MC@NLO results for the differ-

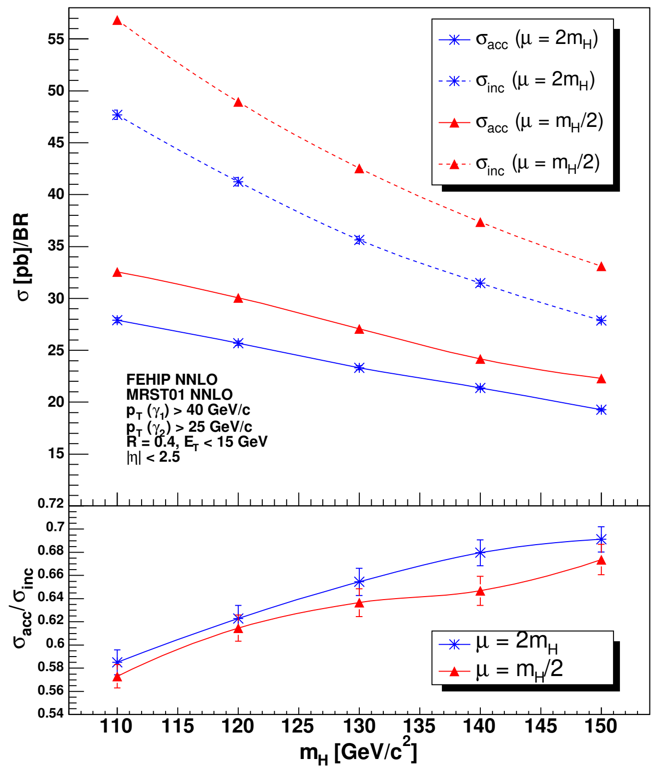

Figure 2: Inclusive and accepted cross sections at NNLO as a function of the Higgs mass, m_{H}, for two different scale choices.

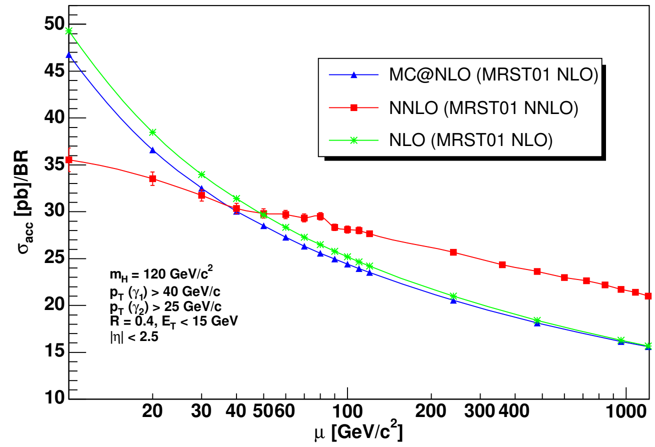

Figure 3: The accepted cross section σ_{acc} predicted by MC@NLO and FEHIP (NLO and NNLO) as a function of the renormalization and factorization scale, μ, for a Higgs mass of $m_{\mathrm{H}} = 120\ \mathrm{GeV}/c^2$.

ent scale choices. Despite the rather large variation of the cross sections when varying μ, the acceptance correction is remarkably stable to within 0.5% (absolute), even when going to scales as low as $m_{\mathrm{H}}/4$. A similar stability of the acceptance correction has been found for single W production at LHC [42].

scale $\mu = \mu_{\mathrm{F}} = \mu_{\mathrm{R}}$	$\mu = m_{\mathrm{h}}/4$	$\mu = m_{\mathrm{h}}/3$	$\mu = m_{\mathrm{h}}/2$	$\mu = m_{\mathrm{h}}$	$\mu = 2m_{\mathrm{h}}$
σ_{inc} [pb]	51.73	47.85	43.30	37.16	32.42

Acceptances ($\sigma_{\mathrm{acc}}/\sigma_{\mathrm{inc}}$) of single groups of cuts					
p_{T}-cuts	80.2 %	80.2 %	80.2 %	80.2 %	80.1 %
η-cuts	83.2 %	83.2 %	83.2 %	83.4 %	83.5 %
isolation	99.7 %	99.7 %	99.7 %	99.8 %	99.8 %

Acceptances ($\sigma_{\mathrm{acc}}/\sigma_{\mathrm{inc}}$) of two groups of cuts					
p_{T}- and η-cuts	63.5 %	63.4 %	63.6 %	63.8 %	63.8 %
p_{T}-cuts and isolation	79.6 %	79.6 %	79.6 %	79.7 %	79.6 %
η-cuts and isolation	81.3 %	81.3 %	81.5 %	81.7 %	81.9 %

All three groups of cuts					
Acceptance	62.9 %	62.8 %	63.0 %	63.3 %	63.4 %
σ_{acc} [pb]	32.52	30.05	27.30	23.53	20.54

Table 3: Acceptance corrections for different cuts and scale choices, as obtained with MC@NLO. The Higgs mass is set to $m_{\mathrm{H}} = 120\ \mathrm{GeV}/c^2$.

5. Differential cross sections

After having calculated the acceptance for a rather standard set of basic selection cuts, it is interesting to investigate further kinematic observables which might help to discriminate the signal from backgrounds. In order to be able to optimize such an additional selection, it is necessary to have a good understanding of the relevant kinematic distributions. Here we concentrate on two observables, which have also been discussed in refs. [27, 22], namely the distributions of the mean of the transverse momenta of the two final state photons $p_{\mathrm{T}}^{\mathrm{m}} = \left(p_{\mathrm{T}}^{\gamma_1} + p_{\mathrm{T}}^{\gamma_2}\right)/2$ and the difference of their pseudo-rapidities $Y^* = |\eta^{\gamma_1} - \eta^{\gamma_2}|/2$. As shown in [27], the latter is interesting since a similar distribution for the prompt photon background is flatter. In the following we focus on a Higgs mass of $m_{\mathrm{H}} = 120\ \mathrm{GeV}/c^2$ and set the renormalization and factorization scale to $\mu = m_{\mathrm{H}}/2$. All the distributions are obtained after applying the selection cuts as described in section 3.

Figure 4 shows the $p_{\mathrm{T}}^{\mathrm{m}}$ (left) and Y^* (right) distributions obtained with MC@NLO when using two different pdf sets, MRST01 NLO and CTEQ6M NLO. We observe that in the interesting region $30\ \mathrm{GeV}/c \leq p_{\mathrm{T}}^{\mathrm{m}} \leq 100\ \mathrm{GeV}/c$ the differential cross section found with CTEQ6M exceeds that obtained with the MRST01 NLO set by up to 5%, in accordance with the differences seen for the inclusive and accepted cross sections listed in table 1. Obviously, the same feature can be found in the Y^* distribution. However, in this case it is remarkable that the ratio of the two predictions is flat over the whole Y^* range, which indicates that the shape of this distribution is rather insensitive to the choice of the pdf set.

The same distributions are reproduced in figure 5, where now the CTEQ6M pdfs have been replaced by those from the MRST01 NNLO set. Similarly to the observations above,

JHEP10(2005)079

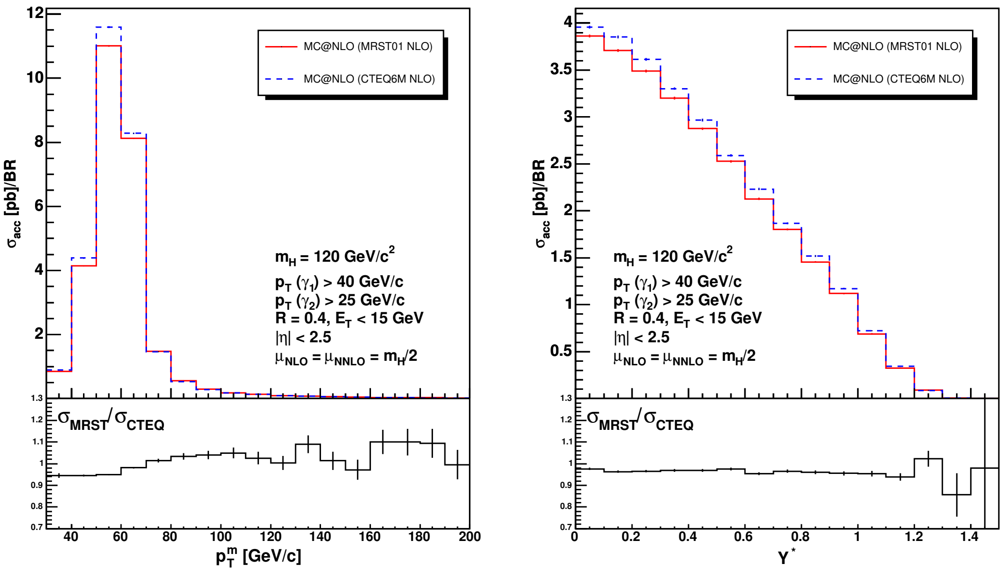

Figure 4: The distributions of the kinematic variables $p_{\mathrm{T}}^{\mathrm{m}}$ (left) and Y^* (right), obtained with MC@NLO for the two pdf sets MRST01 NLO and CTEQ6M NLO. The standard cuts as indicated in the plots have been applied.

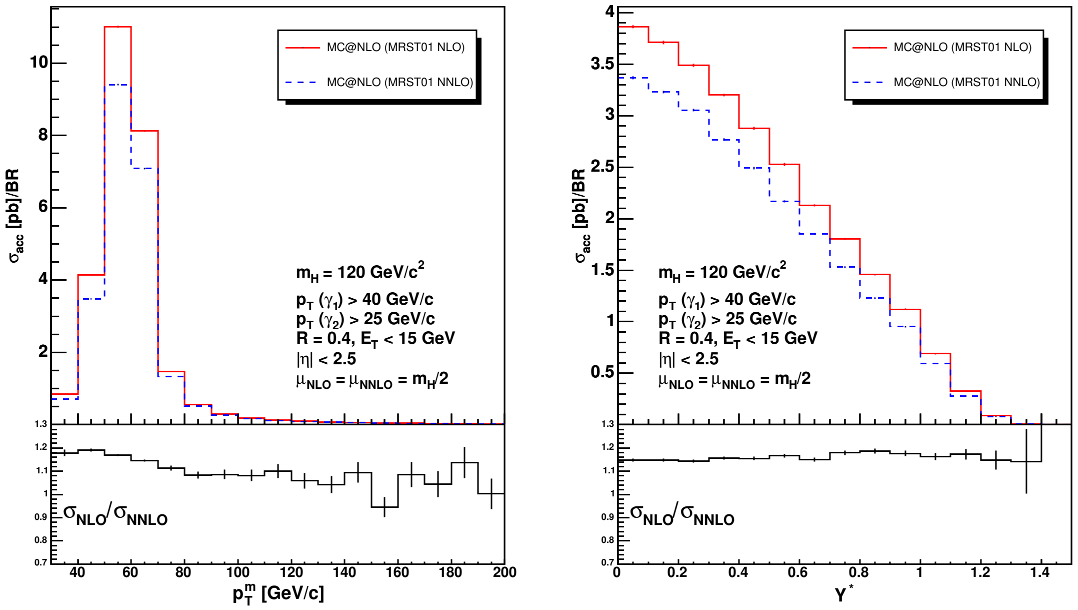

Figure 5: The distributions of the kinematic variables $p_{\mathrm{T}}^{\mathrm{m}}$ (left) and Y^* (right), obtained with MC@NLO for the two pdf sets MRST01 NLO and MRST01 NNLO. The standard cuts as indicated in the plots have been applied.

the shapes of the two histograms differ only slightly, in particular in the case of Y^*, with the results based on the NNLO pdfs being lower than those from the NLO set. This has been discussed previously, cf. section 4.1 and table 1. Thus the assumption is confirmed that the choice of the pdf set does not strongly affect the shape of these distributions.

JHEP10(2005)079

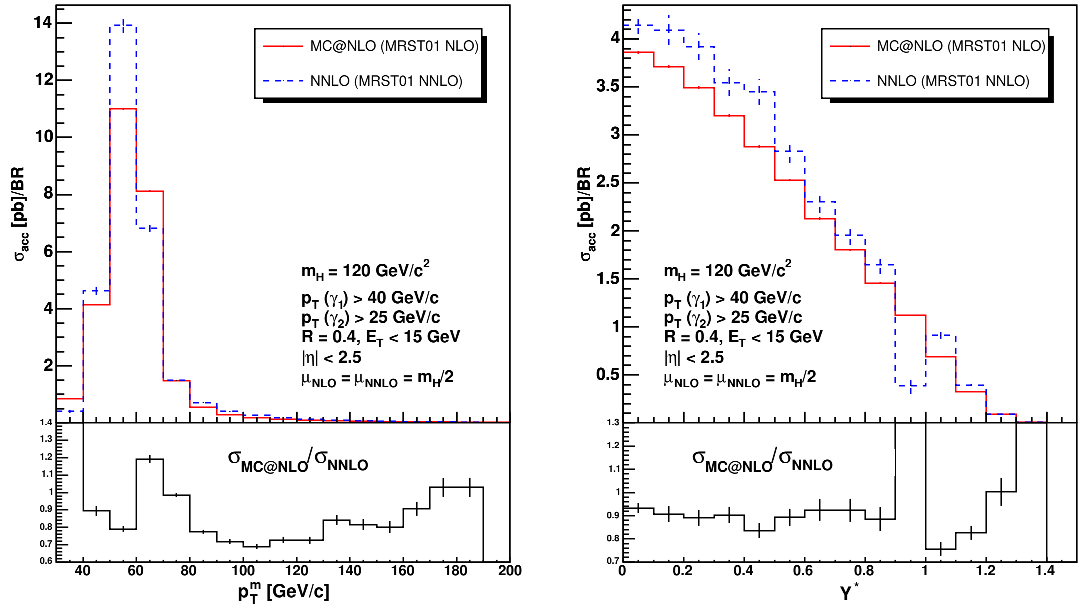

Figure 6: The distributions of the kinematic variables p_T^m (left) and Y^* (right), obtained with MC@NLO (pdf set MRST01 NLO) and FEHIP (NNLO). The standard cuts as indicated in the plots have been applied.

Finally, in figure 6 we compare the distributions obtained with MC@NLO and with FEHIP at NNLO. Concerning the variable p_T^m, we observe that in the peak region the shapes of the distributions differ rather strongly, with the maximum shifted to lower values when going from MC@NLO to NNLO. The appearance of these large perturbative corrections close to the kinematic boundary has also been discussed in [22]. From the upper tail, thus far beyond this boundary, it is evident that at larger photon momenta the cross section is higher at NNLO with respect to MC@NLO. Regarding the Y^* distribution it is particularly interesting to observe that the step in the NNLO prediction around $Y^* = 0.9 - 1.0$ does not appear for MC@NLO. Such a step is typical for fixed order calculations when a phase-space boundary varies at different orders in the perturbation series, however, it can be removed by the inclusion of soft-gluon resummation to all orders [43]. In the case of Y^*, the leading order cross section is zero above $Y^* = 0.96$.

6. Comparison to the irreducible background

After having analyzed the signal cross sections as functions of the measurable final state photon momenta, it is natural to compare these differential results to those for the irreducible background, namely prompt photon production, pp $\to \gamma\gamma + X$. The latter have been computed with DIPHOX [28] at NLO (cf. section 2), with MRST01 NLO as pdf set. The renormalization and factorization scales are fixed to $\mu = m_{\rm H}/2$ for the signal, computed with MC@NLO, and $\mu = m_{\gamma\gamma}/2$ for the background, where $m_{\gamma\gamma}$ is the invariant mass of the two final-state photons. For the photon fragmentation we use the NLO fragmentation functions (set I) from [44].

JHEP10(2005)079

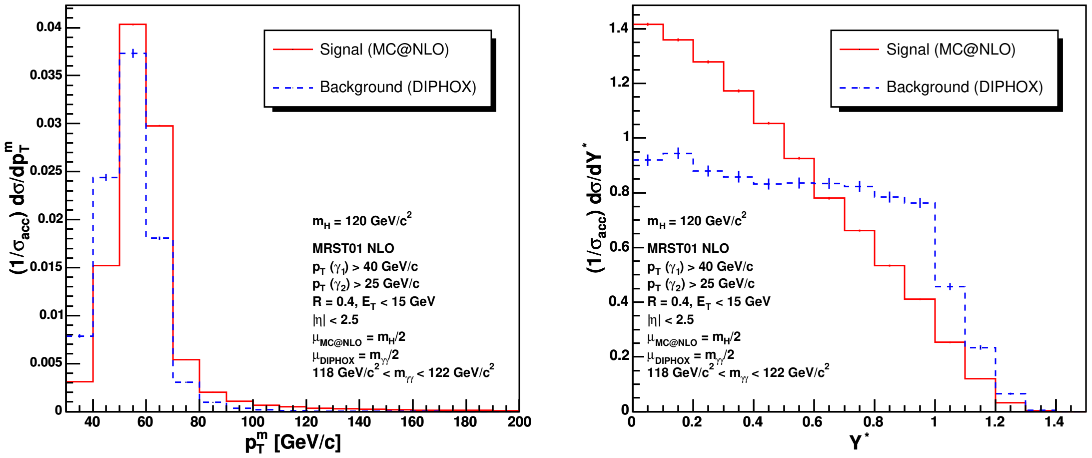

Figure 7: Normalized distributions of p_T^{m} (left) and Y^* (right) for signal and background. The standard cuts as indicated in the plots have been applied.

Figure 7 compares the normalized distributions of p_T^{m} (left) and Y^* (right) for signal and background. For the background, only events with 118 GeV$/c^2 \leq m_{\gamma\gamma} \leq$ 122 GeV$/c^2$ are included, corresponding to a mass-window of ± 2 GeV$/c^2$ around the Higgs mass $m_{\mathrm{H}} =$ 120 GeV$/c^2$. As expected, the shapes differ considerably. In the case of p_T^{m}, the mean is clearly shifted towards lower values for the background. The Y^* distribution offers an even better handle for the signal-background discrimination, since the background is rather flat, whereas the signal is peaked for small values of Y^*.

6.1 Statistical significance

In table 4 we compare the signal cross section obtained with MC@NLO to the background cross section computed with DIPHOX. Here, σ_{inc} refers to the inclusive pp $\to$H $\to\gamma\gamma + X$ cross section before any cut. In addition to the acceptance correction found with MC@NLO (cf. section 4), we also account for a photon reconstruction efficiency of 57% as was done in ref. [27], corresponding to a combination of 81% for γ/jet identification per photon and 87% for fiducial cuts. The branching ratio for the Higgs decay channel into two photons is calculated with HDECAY. Altogether this gives an effective signal cross section of $\sigma_{\mathrm{eff}} = 0.034$ pb. If we assume an integrated luminosity of 30 fb^{-1}, corresponding to about three years of LHC running at low luminosity, we find a total number of $S = 1027$ signal events.

In order to calculate the number of background events, we only consider events with a total invariant mass of the two final-state photons between 118 and 122 GeV$/c^2$. In this case, the cross section after cuts amounts to $\sigma_{\mathrm{acc}} = 0.944$ pb, as shown in the right column of table 4. In addition to the efficiency factor, we include a 20% reducible background [27]. This leads to an effective background cross section of $\sigma_{\mathrm{eff}} = 0.631$ pb and to a total number of $B = 18928$ background events. Thus, we end up with a significance of $S/\sqrt{B} = 7.5$.

A few remarks are in place here. First, this is the significance obtained only after applying the basic selection cuts given in section 3, without any further signal-background

JHEP10(2005)079

$\mathrm{pp} \to \gamma\gamma + X$			
Signal		Background	
σ_{inc} [pb]	43.30		
acceptance	63.0 %		
σ_{acc} [pb]	27.30	σ_{acc} [pb]	0.9244
efficiency factor	57 %	efficiency factor	57 %
branching ratio	0.22 %	other reducible background	20 %
σ_{eff} [pb]	0.034	σ_{eff} [pb]	0.631
int. luminosity [fb^{-1}]	30	int. luminosity [fb^{-1}]	30
number of events S	1027	number of events B	18928
significance $S/\sqrt{B} = 7.5$			

Table 4: Accepted number of signal and background events after applying standard selection cuts and corresponding significance $S/\sqrt{B}$ for a Higgs mass of $m_{\mathrm{H}} = 120$ GeV/c^2.

discrimination as suggested, eg. by the observations from figure 7. Second, DIPHOX does not contain the two-loop correction to the gluon fusion subprocess of $\mathrm{pp} \to \gamma\gamma + X$, which has been calculated in [27]. However, its inclusion would only lead to a 5% reduction of the statistical significance given in table 4. Furthermore, it is worth noting that the background has been calculated at NLO, while the signal obtained with MC@NLO includes corrections beyond that order. We think that a calculation of the prompt photon background to such an approximation as can be obtained with the MC@NLO approach would be highly desirable, both from the phenomenological and experimental point of view.

7. Summary

We have analyzed perturbative QCD predictions at and beyond next-to-leading order accuracy for the Higgs production and decay in the channel $\mathrm{pp} \to \mathrm{H} \to \gamma\gamma + X$ at LHC energies. In particular, for the first time it has become possible to compare the results from the MC@NLO Monte Carlo generator to a full NNLO prediction, not only for inclusive cross sections, but also for the accepted cross sections obtained after applying standard selection cuts.

Whereas the inclusive and accepted cross sections at NLO and NNLO differ by about 10%, it turns out that the acceptance corrections agree to within 2%. The latter are also very stable under variations of the renormalization and factorization scale and rather insensitive to the choice of the parton distribution functions. This is not the case when looking at the cross section themselves, in particular at NLO approximation.

We have also analyzed distributions of kinematic observables constructed from the final-state photon momenta, namely the average of the two photon transverse momenta and their rapidity difference. Some differences in the shapes of the distributions have been found between MC@NLO and the exact NNLO calculation. More importantly, it has been shown that these distributions should allow for a good discrimination between the Higgs signal and the irreducible prompt photon background.

JHEP10(2005)079

Acknowledgments

We would like to warmly thank K. Melnikov, F. Petriello and in particular C. Anastasiou for the many and very interesting discussions, for the help with the FEHIP code and the comments on the manuscript. Furthermore we are grateful to S. Frixione and B. Webber for their feedback on our questions related to MC@NLO, as well as for the useful comments on the manuscript. We thank M. Spira for his advice on issues regarding the theory of Higgs production.

References

[1] T. Hambye and K. Riesselmann, *SM Higgs mass bounds from theory*, hep-ph/9708416.

[2] G. Altarelli and M.W. Grunewald, *Precision electroweak tests of the standard model*, *Phys. Rept.* **403-404** (2004) 189 [hep-ph/0404165].

[3] ATLAS collaboration, *ATLAS detector and physics performance: technical design report vol. 2*, CERN-LHCC-99-15.

[4] CMS collaboration, *The electromagnetic calorimeter project: technical design report*, CERN-LHCC-97-33.

[5] S. Abdullin et al., *Summary of the CMS potential for the Higgs boson discovery*, *Eur. Phys. J.* **C 39S2** (2005) 41.

[6] S. Dawson, *Radiative corrections to Higgs boson production*, *Nucl. Phys.* **B 359** (1991) 283.

[7] A. Djouadi, M. Spira and P.M. Zerwas, *Production of Higgs bosons in proton colliders: QCD corrections*, *Phys. Lett.* **B 264** (1991) 440.

[8] D. Graudenz, M. Spira and P.M. Zerwas, *QCD corrections to Higgs boson production at proton proton colliders*, *Phys. Rev. Lett.* **70** (1993) 1372.

[9] M. Spira, A. Djouadi, D. Graudenz and P.M. Zerwas, *Higgs boson production at the LHC*, *Nucl. Phys.* **B 453** (1995) 17 [hep-ph/9504378].

[10] S. Catani, D. de Florian and M. Grazzini, *Higgs production in hadron collisions: soft and virtual QCD corrections at NNLO*, *JHEP* **05** (2001) 025 [hep-ph/0102227].

[11] R.V. Harlander and W.B. Kilgore, *Soft and virtual corrections to* $\mathrm{pp} \to H + X$ *at NNLO*, *Phys. Rev.* **D 64** (2001) 013015 [hep-ph/0102241].

[12] R.V. Harlander and W.B. Kilgore, *Next-to-next-to-leading order Higgs production at hadron colliders*, *Phys. Rev. Lett.* **88** (2002) 201801 [hep-ph/0201206].

[13] C. Anastasiou and K. Melnikov, *Higgs boson production at hadron colliders in NNLO QCD*, *Nucl. Phys.* **B 646** (2002) 220 [hep-ph/0207004].

[14] V. Ravindran, J. Smith and W.L. van Neerven, *NNLO corrections to the total cross section for Higgs boson production in hadron hadron collisions*, *Nucl. Phys.* **B 665** (2003) 325 [hep-ph/0302135].

[15] S. Moch and A. Vogt, *Higher-order soft corrections to lepton pair and Higgs boson production*, hep-ph/0508265.

[16] G. Degrassi and F. Maltoni, *Two-loop electroweak corrections to Higgs production at hadron colliders*, *Phys. Lett.* **B 600** (2004) 255 [hep-ph/0407249].

[17] G. Degrassi and F. Maltoni, *Two-loop electroweak corrections to the Higgs-boson decay H* $\rightarrow \gamma\gamma$, hep-ph/0504137.

[18] D. de Florian, M. Grazzini and Z. Kunszt, *Higgs production with large transverse momentum in hadronic collisions at next-to-leading order*, *Phys. Rev. Lett.* **82** (1999) 5209 [hep-ph/9902483].

[19] V. Ravindran, J. Smith and W.L. Van Neerven, *Next-to-leading order QCD corrections to differential distributions of Higgs boson production in hadron hadron collisions*, *Nucl. Phys.* **B 634** (2002) 247 [hep-ph/0201114].

[20] G. Davatz, G. Dissertori, M. Dittmar, M. Grazzini and F. Pauss, *Effective K-factors for* $gg \rightarrow H \rightarrow WW \rightarrow \ell\nu\ell\nu$ *at the LHC*, *JHEP* **05** (2004) 009 [hep-ph/0402218].

[21] C. Anastasiou, K. Melnikov and F. Petriello, *Higgs boson production at hadron colliders: differential cross sections through next-to-next-to-leading order*, *Phys. Rev. Lett.* **93** (2004) 262002 [hep-ph/0409088].

[22] C. Anastasiou, K. Melnikov and F. Petriello, *Fully differential Higgs boson production and the di-photon signal through next-to-next-to-leading order*, hep-ph/0501130.

[23] S. Frixione and B.R. Webber, *Matching NLO QCD computations and parton shower simulations*, *JHEP* **06** (2002) 029 [hep-ph/0204244].

[24] S. Frixione, P. Nason and B.R. Webber, *Matching NLO QCD and parton showers in heavy flavour production*, *JHEP* **08** (2003) 007 [hep-ph/0305252].

[25] G. Corcella et al., *Herwig 6: an event generator for hadron emission reactions with interfering gluons (including supersymmetric processes)*, *JHEP* **01** (2001) 010 [hep-ph/0011363].

[26] G. Corcella et al., *Herwig 6.5 release note*, hep-ph/0210213.

[27] Z. Bern, L.J. Dixon and C. Schmidt, *Isolating a light Higgs boson from the di-photon background at the LHC*, *Phys. Rev.* **D 66** (2002) 074018 [hep-ph/0206194].

[28] T. Binoth, J.P. Guillet, E. Pilon and M. Werlen, *A full next to leading order study of direct photon pair production in hadronic collisions*, *Eur. Phys. J.* **C 16** (2000) 311 [hep-ph/9911340].

[29] A.D. Martin, R.G. Roberts, W.J. Stirling and R.S. Thorne, *NNLO global parton analysis*, *Phys. Lett.* **B 531** (2002) 216 [hep-ph/0201127].

[30] C. Anastasiou, K. Melnikov, and F. Petriello, private communication.

[31] R. Kreckel, *Parallelization of adaptive MC integrators*, *Comput. Phys. Commun.* **106** (1997) 258, physics/9710028.

[32] R. Kreckel, *Parallelization of adaptive MC integrators — recent pvegas developments*, physics/9812011.

[33] *MPI: A message-passing interface standard*, University of Tennessee, Knoxville, Tennessee (1995), see http://www-unix.mcs.anl.gov/mpi/.

[34] S. Frixione, private communication.

[35] J. Pumplin et al., *New generation of parton distributions with uncertainties from global QCD analysis*, *JHEP* **07** (2002) 012 [hep-ph/0201195].

JHEP10(2005)079

[36] A. Djouadi, J. Kalinowski and M. Spira, *HDECAY: a program for Higgs boson decays in the standard model and its supersymmetric extension*, *Comput. Phys. Commun.* **108** (1998) 56 [hep-ph/9704448].

[37] M. Spira, *HIGLU: a program for the calculation of the total Higgs production cross section at hadron colliders via gluon fusion including QCD corrections*, hep-ph/9510347.

[38] ATLAS collaboration, *ATLAS: Letter of intent for a general purpose pp experiment at the Large Hadron Collider at CERN*, CERN-LHCC-92-4.

[39] CMS collaboration, *CMS: The Compact Muon Solenoid: Letter of intent for a general purpose detector at the LHC*, CERN-LHCC-92-3.

[40] S. Frixione, *Isolated photons in perturbative QCD*, *Phys. Lett.* **B 429** (1998) 369 [hep-ph/9801442].

[41] S. Catani, D. de Florian, M. Grazzini and P. Nason, *Soft-gluon resummation for Higgs boson production at hadron colliders*, *JHEP* **07** (2003) 028 [hep-ph/0306211].

[42] S. Frixione and M.L. Mangano, *How accurately can we measure the W cross section?*, *JHEP* **05** (2004) 056 [hep-ph/0405130].

[43] S. Catani and B.R. Webber, *Infrared safe but infinite: soft-gluon divergences inside the physical region*, *JHEP* **10** (1997) 005 [hep-ph/9710333].

[44] L. Bourhis, M. Fontannaz and J.P. Guillet, *Quark and gluon fragmentation functions into photons*, *Eur. Phys. J.* **C 2** (1998) 529 [hep-ph/9704447].

JHEP10(2005)079